雑誌

発表者氏名	論文タイトル名	発表誌名	巻号	ページ	出版年
Tateno A, Sakayori T, Kawashima Y, Higuchi M, Suhara T, Mizumura S, Honjo K, Mintun MA, Skovronsky DM, Okubo Y.	Comparison of imaging biomarkers for Alzheimer's disease: amyloid imaging with florbetapir F18 positron emission tomography and MRI voxel-based analysis for entorhinal cortex atrophy.	Int J Geriatr Psychiatry		in press.	
Tateno A, Sakayori T, Higuchi M, Suhara T, Honjo K, Ishihara K, Kumita S, Suzuki H, Okubo Y.	Amyloid imaging with [18F]florbetapir in geriatric depression: early-onset versus late-onset.	Int J Geriatr Psychiatry		in press	
Tateno A, Sakayori T, Takizawa Y, Yamamoto K, Minagawa K, Okubo Y.	A case of Alzheimer's disease following mild traumatic brain injury.	Gen Hosp Psychiatry		in press	
Kim WC, Tateno A, Arakawa R, Sakayori T, Ikeda Y, Suzuki H, Okubo Y. Int J	In vivo activity of modafinil on dopamine transporter measured with positron emission tomography and [18F] FE-PE2I.	Neuropsychopharmacol	17(5)	697-703	2014
Koeda M, Watanabe A, Tsuda K, Matsumoto M, Ikeda Y, Kim W, Tateno A, Naing BT, Karibe H, Shimada T, Suzuki H, Matsuura M, Okubo Y. 2015	Interaction effect between handedness and CNTNAP2 polymorphism (rs7794745 genotype) on voice-specific frontotemporal activity in healthy individuals: an fMRI study.	Front Behav Neurosci.		in press	2015
Ueda S, Omori A, Shioya T, Okubo Y.	Antipsychotics can induce pre-shock in very elderly patients: a report of two cases.	Psychogeriatrics.		in press	2015
Shimoda K, Kimura M, Yokota M, Okubo Y.	Comparison of regional gray matter volume abnormalities in Alzheimer?s disease and late life depression with hippocampal atrophy using VSRAD analysis: A voxel-based morphometry study.	Psychiatry Res.		in press	2015

Kurita M, Nishino S, Numata Y, Okubo Y, Sato T.	The noradrenaline metabolite MHPG is a candidate biomarker between the depressive, remission, and manic states in bipolar disorder I: two long-term naturalistic case reports.	Neuropsychiatr Dis Treat.		in press	2015
Kurita M, Nishino S, Numata Y, Okubo Y, Sato T. clinical naturalistic	The noradrenaline metabolite MHPG is a candidate biomarker from the manic to the remission state in bipolar disorder I: a study..	PLoS One.	9(6)	e100634.	2014
Endo T, Saijo T, Haneda E, Maeda J, Tokunaga M, Zang MR, Kannami A, Asai H, Suzuki M, Suhara T, Higuchi M	Quantification of central substance P receptor occupancy by aprepitant using small animal positron emission tomography.	Int J Neuropsychopharmacol	18(2)	1-10	2015
Chen CJ, Bando K, Ashino H, Taguchi K, Shiraishi H, Shima K, Fujimoto O, Kitamura C, Matsushima S, Uchida K, Nakahara Y, Kasahara H, Minamizawa T, Jiang C, Zhang MR, Ono M, Tokunaga M, Suhara T, Higuchi M, Yamada K, Ji B	In Vivo SPECT Imaging of Amyloid-β Deposition with Radioiodinated Imidazo[1,2-α]pyridine Derivative DRM106 in Mouse Model of Alzheimer's Disease.	J Nucl Med	56(1)	120-126	2015
Hashimoto H, Kawamura K, Igarashi N, Takei M, Fujishiro T, Aihara Y, Shiomi S, Muto M, Ito T, Furutsuka K, Yamasaki T, Yui J, Xie L, Ono M, Hatori A, Nemoto K, Suhara T, Higuchi M, Zhang MR	Radiosynthesis, Photoisomerization, Biodistribution, and Metabolite Analysis of ^{11}C-PBB3 as a Clinically Useful PET Probe for Imaging of Tau Pathology.	J Nucl Med	55(9)	1532-1538	2014
Sahara N, Murayama M, Higuchi M, Suhara T, Takashima A	Biochemical Distribution of Tau Protein in Synaptosomal Fraction of Transgenic Mice Expressing Human P301L Tau.	Front Neurol	5	26	2014

Ito H, Shinotoh H, Shimada H, Miyoshi M, Yanai K, Okamura N, Takano H, Takahashi H, Arakawa R, Kodaka F, Ono M, Eguchi Y, Higuchi M, Fukumura T, Suhara T	Imaging of amyloid deposition in human brain using positron emission tomography and [^{18}F]FACT: comparison with [^{11}C]PIB.	Eur J Nucl Med Mol Imaging	41(4)	745-754	2014
Chen CJ, Bando K, Ashino H, Taguchi K, Shiraishi H, Shima K, Fujimoto O, Kitamura C, Morimoto Y, Kasahara H, Minamizawa T, Jiang C, Zhang MR, Suhara T, Higuchi M, Yamada K, Ji B	Biological evaluation of the radioiodinated imidazo[1,2-a]pyridine derivative DRK092 for amyloid-β imaging in mouse model of Alzheimer's disease.	Neurosci Lett	581	103-108	2014
Chen CJ, Bando K, Ashino H, Taguchi K, Shiraishi H, Fujimoto O, Kitamura C, Matsushima S, Fujinaga M, Zhang MR, Kasahara H, Minamizawa T, Jiang C, Ono M, Higuchi M, Suhara T, Yamada K, Ji B	Synthesis and biological evaluation of novel radioiodinated imidazopyridine derivatives for amyloid-β imaging in Alzheimer's disease.	Bioorg Med Chem	22(15)	4189-4197	2014
Ito H, Shimada H, Shinotoh H, Takano H, Sasaki T, Nogami T, Suzuki M, Nagashima T, Takahata K, Seki C, Kodaka F, Eguchi Y, Fujiwara H, Kimura Y, Hirano S, Ikoma Y, Higuchi M, Kawamura K, Fukumura T, Böö EL, Farde L, Suhara T	Quantitative Analysis of Amyloid Deposition in Alzheimer Disease Using PET and the Radiotracer ^{11}C-AZD2184.	J Nucl Med	55(6)	932-938	2014
Hajime Tabuchi, Mika Konishi, Fumie Saito, Motoichiro Kato, Masaru Mimura.	Reverse Fox Test for Detecting Visuospatial Dysfunction Corresponding to Parietal Hypoperfusion in Mild Alzheimer's disease.	Am J Alzheimers Dis Other Demen.	29(2)	177-182	2014

Miki Bundo, Manabu Toyoshima, Junko Ueda, Taeko Nemoto-Miyauchi, Fumiko Sunaga, Michihiro Toritsuka, Daisuke Ikawa, Akiyoshi Kakita, Yohei Okada, Wado Akamatsu, Motoichiro Kato, Hideyuki Okano, Kiyoto Kasai, Toshifumi Kishimoto, Hiroyuki Nawa, Takeo Yoshikawa, Tadafumi Kato, Kazuya Iwamoto.	Increased L1 Retrotransposition in the Neuronal Genome in Schizophrenia.	Neuron	81	:306-313,	2014
Mitsuhiro Sado, Joichiro Shirahase, Kimio Yoshimura, Yuki Miura, Kazuhiro Yamamoto, Hajime Tabuchi, Motoichiro Kato, Masaru Mimura.	Predictors of repeated sick leave in the workplace because of mental disorders.	Neuropsychiatric Disease and Treatment	10	193-200	2014
Keisuke Takahata, Fumie Saito, Taro Muramatsu, Makiko Yamada, Joichiro Shirahase, Hajime Tabuchi1, Tetsuya Suhara, Masaru Mimura, Motoichiro Kato*	: Emergence of realism:Enhanced visual artistry and high accuracy of visual numerosity representation after left prefrontal damage .	Neuropsychologia	57	28-49,	:2014
Motoko Maekawa, Kazuo Yamada, Manabu Toyoshima, Tetsuo Ohnishi, Yoshimi Iwayama, Chie Shimamoto, Tomoko Toyota, Yayoi Nozaki, Shabeesh Balan, Hideo Matsuzaki, Yasuhide Iwata, Katsuaki Suzuki, Mitsuhiro Miyashita, MitsuruKikuchi, Motoichiro Kato, Yohei Okada, Wado Akamatsu, Norio Mori, Yuji Owada, Masanari Itokawa, Hideyuki Okano, Takeo Yoshikawa.	Utility of Scalp Hair Follicles as a Novel Source of Biomarker Genes for Psychiatric Illnesses.	Biological Psychiatry,	3223(14)	00570-8	2014

Fujino J, Yamasaki N, Miyata J, Kawada R, Sasaki H, Matsukawa N, Takemura A, Ono M, Tei S, Takahashi H, Aso T, Fukuyama H, Murai T.	Altered brain response to others' pain in major depressive disorder.	J Affect Disord.	165	170-5	2014
Tei S, Becker C, Kawada R, Fujino J, Jankowski K, Sugihara G, Murai T, Takahashi H.	Can we predict burnout severity from empathy-related brain activity?	Transl Psychiatry	4	e393	2014
Tei S, Becker C, Sugihara G, Kawada R, Fujino J, Sozu T, Murai T, Takahashi H.	Sense of meaning in work and risk of burnout among medical professionals.	Psychiatry Clin Neurosci.	69(2)	123-4	2015
Fujino J, Yamasaki N, Miyata J, Sasaki H, Matsukawa N, Takemura A, Tei S, Sugihara G, Aso T, Fukuyama H, Takahashi H, Inoue K, Murai T.	Anterior cingulate volume predicts response to cognitive behavioral therapy in major depressive disorder.	J Affect Disord.	174	397-9	2015
Tanaka Y, Fujino J, Ideno T, Okubo S, Takemura K, Miyata J, Kawada R, Fujimoto S, Kubota M, Sasamoto A, Hirose K, Takeuchi H, Fukuyama H, Murai T, Takahashi H.	Are ambiguity aversion and ambiguity intolerance identical? A neuroeconomics investigation.	Front Psychol.	5	1550	2015
Fujino J, Yamasaki N, Miyata J, Kawada R, Sasaki H, Matsukawa N, Takemura A, Ono M, Tei S, Takahashi H, Aso T, Fukuyama H, Murai T.	Altered brain response to others' pain in major depressive disorder.	J Affect Disord.	165	170-5	2014

Ⅳ. 研究成果の刊行物・別刷

RESEARCH ARTICLE

International Journal of Geriatric Psychiatry

Comparison of imaging biomarkers for Alzheimer's disease: amyloid imaging with [^{18}F]florbetapir positron emission tomography and magnetic resonance imaging voxel-based analysis for entorhinal cortex atrophy

Amane Tateno[1], Takeshi Sakayori[1], Yoshitaka Kawashima[1], Makoto Higuchi[2], Tetsuya Suhara[2], Sunao Mizumura[3], Mark A. Mintun[4], Daniel M. Skovronsky[4], Kazuyoshi Honjo[5], Keiichi Ishihara[5], Shinichiro Kumita[6], Hidenori Suzuki[7] and Yoshiro Okubo[1]

[1]Department of Neuropsychiatry, Nippon Medical School, 1-1-5 Sendagi, Bunkyo-ku, Tokyo, Japan
[2]Molecular Imaging Center, National Institute of Radiological Sciences, 4-9-1 Anagawa, Inage-ku, Chiba, Japan
[3]Department of Radiology, Toho University Omori Medical Center, 6-11-1 Omori-nishi, Ota-ku, Tokyo, Japan
[4]Avid Radiopharmaceuticals, Inc., 3711 Market St., 7th Floor, Philadelphia, PA 19104, USA
[5]Clinical Imaging Center for Healthcare, Nippon Medical School, Sendagi 1-12-15, Bunkyo-ku, Tokyo, Japan
[6]Department of Radiology, Nippon Medical School, 1-1-5 Sendagi, Bunkyo-ku, Tokyo, Japan
[7]Department of Pharmacology, Nippon Medical School, 1-1-5 Sendagi, Bunkyo-ku, Tokyo, Japan
Correspondence to: Yoshiro Okubo, E-mail: okubo-y@nms.ac.jp

Objective: We compared amyloid positron emission tomography (PET) and magnetic resonance imaging (MRI) in subjects clinically diagnosed with Alzheimer's disease (AD), mild cognitive impairment (MCI), and older healthy controls (OHC) in order to test how these imaging biomarkers represent cognitive decline in AD.

Methods: Fifteen OHC, 19 patients with MCI, and 19 patients with AD were examined by [^{18}F]florbetapir PET to quantify the standard uptake value ratio (SUVR) as the degree of amyloid accumulation, by MRI and the voxel-based specific regional analysis system for AD to calculate *z*-score as the degree of entorhinal cortex atrophy, and by mini-mental state examination (MMSE) and Alzheimer's Disease Assessment Scale–cognitive component—Japanese version (ADAS-Jcog) for cognitive functions.

Results: Both cutoff values for measuring AD-like levels of amyloid (1.099 for SUVR) and entorhinal cortex atrophy (1.60 for *z*-score) were well differentially diagnosed and clinically defined AD from OHC (84.2% for SUVR and 86.7% for *z*-score). Subgroup analysis based on beta-amyloid positivity revealed that *z*-score significantly correlated with MMSE ($r = -0.626$, $p < 0.01$) and ADAS-Jcog ($r = 0.691$, $p < 0.01$) only among subjects with beta-amyloid.

Conclusions: This is the first study to compare [^{18}F]florbetapir PET and MRI voxel-based analysis of entorhinal cortex atrophy for AD. Both [^{18}F]florbetapir PET and MRI detected changes in AD compared with OHC. Considering that entorhinal cortex atrophy correlated well with cognitive decline only among subjects with beta-amyloid, [^{18}F]florbetapir PET makes it possible to detect AD pathology in the early stage, whereas MRI morphometry for subjects with beta-amyloid provides a good biomarker to assess the severity of AD in the later stage. Copyright © 2014 John Wiley & Sons, Ltd.

Key words: Alzheimer's disease; beta-amyloid; positron emission tomography; brain atrophy; cognitive function
History: Received 2 April 2014; Accepted 6 June 2014; Published online 7 July 2014 in Wiley Online Library (wileyonlinelibrary.com)
DOI: 10.1002/gps.4173

Introduction

Both beta-amyloid and tau proteins play significant roles in the process of Alzheimer's disease (AD). Technological progress has allowed us to visualize the distribution of these proteins *in vivo*. Imaging of tau was newly developed (Maruyama *et al.*, 2013), and future research is expected to benefit greatly. On the other hand, the imaging of beta-amyloid has led to the accumulation of much scientific knowledge. Development of [^{11}C] Pittsburgh compound-B (Klunk *et al.*, 2004) from thioflavin T for positron emission tomography (PET) enabled the detection of beta-amyloid *in vivo*. Since then, amyloid PET studies have provided much valuable information about AD, such as that patients clinically diagnosed as AD had significantly more beta-amyloid than healthy controls (Kemppainen *et al.*, 2006), and the presence of beta-amyloid detected by amyloid PET might predict mild cognitive impairment (MCI) conversion to AD (Rinne and Någren, 2010). Nowadays, it is well accepted that PET can detect beta-amyloid *in vivo* to the same extent as postmortem histopathology.

For florbetapir PET, thresholds were created by automatically characterized cerebral-to-whole-cerebellar standard uptake value ratios (SUVRs) and diagnosis of AD by autopsy (Fleisher *et al.*, 2011). The same florbetapir PET study reported that the percentage of positive beta-amyloid was 85.3% for patients with clinically diagnosed AD, 46.6% for patients with MCI, and 28.1% for older healthy controls (OHC) (Fleisher *et al.*, 2011). Another study also reported highly significant correlations between the results from florbetapir PET and subsequent immunohistochemistry measurements of fibrillar beta-amyloid, with the results of florbetapir PET and postmortem rated as positive or negative for beta-amyloid showing 96% agreement (Clark *et al.*, 2011). These findings might equally apply to the Japanese population, but there has been no study using florbetapir PET in Japan.

The volume reductions of specific brain regions provide useful information for diagnosing dementia. A previous study reported sensitivity and specificity of brain atrophy in the medial temporal lobe of 85% and 88% among patients with clinically diagnosed AD and normal (Scheltens *et al.*, 2002), but it is often difficult to evaluate mild atrophy by visual inspection of magnetic resonance imaging (MRI). The voxel-based specific regional analysis system for AD (VSRAD) was recently developed as a sensitive diagnostic tool for early stages of AD (Hirata *et al.*, 2005; Matsuda *et al.*, 2012). VSRAD is software that automatically analyzes three-dimensional T_1-weighted MRI and quantifies the medial temporal volumes targeting the entorhinal cortex. Recent studies reported that VSRAD showed a high accuracy of 87.8% in the discrimination of patients with clinically diagnosed AD in the very early stage from control (Hirata *et al.*, 2005), that the degree of atrophy evaluated by VSRAD was associated with the severity of executive dysfunction (Nagata *et al.*, 2011), and that VSRAD was useful for both early-onset and late-onset AD (Shibuya *et al.*, 2013). According to the hypothetical model of dynamic biomarkers in relation to the disease stage of AD, accumulation of beta-amyloid occurs early in the disease, before the appearance of clinical symptoms, and brain atrophy detected by MRI is related closely to cognitive performance and is the last biomarker to become abnormal (Jack *et al.*, 2010). A few studies have investigated the association between beta-amyloid deposition and cortical thinning or atrophy (Jack *et al.*, 2008; Becker *et al.*, 2011). However, no study has directly compared how these different imaging biomarkers differentially diagnosed clinical AD from healthy subjects using a group of the same subjects.

In the present study, we examined how these different imaging techniques, amyloid imaging with [^{18}F] florbetapir PET and entorhinal cortex volume analysis with VSRAD, differentially diagnosed clinically defined AD from healthy control. We also compared the different imaging biomarkers in terms of association with cognitive decline.

Material and methods

Subjects and study protocol

Participants were recruited between May 2010 and August 2012. The study population consisted of Japanese men and women with clinically diagnosed AD, MCI, and OHC without cognitive impairment. OHC were 65 years of age or older. They were required to be without subjective cognitive complaints as corroborated by an informant report, to have mini-mental state examination (MMSE) (Folstein *et al.*, 1975) score of 27 or higher, and to be cognitively normal based on psychometric testing. The clinical diagnosis of AD (clinical AD) was based on the 1984 edition of the NINCDS-ADRDA criteria (McKhann *et al.*, 1984). Patients with clinical AD at least met the criteria of probable AD. Participants with MCI were 55 years old or older and had complaints of memory or cognitive decline corroborated by an informant, objective cognitive impairment, generally preserved functional abilities and activity of daily living (ADL), a Clinical Dementia Rating (CDR) (Morris, 1993) scale global score higher than 0, an MMSE score

higher than 23, and no diagnosis of dementia at screening. All neuropsychological tests were performed by Y. K., who was blinded to the results of imaging data and diagnosis.

Participants were excluded if they had other current clinically relevant neurologic illness or history of apparent brain injury, were receiving any investigational medications, or had ever received anti-amyloid experimental therapy. In this study, the participants were 15 OHC, 19 patients with clinical AD, and 19 patients with MCI. Fifteen of 19 AD patients and three of 19 MCI patients took anti-dementia drugs (17 subjects took donepezil and one took galantamine). Their cognitive function was evaluated by MMSE and the Alzheimer's Disease Assessment Scale–cognitive component—Japanese version (ADAS-Jcog) (Homma *et al.*, 1992). Their ADL was measured by CDR. Their behavioral and psychological symptoms of dementia were examined by the Neuropsychiatric Inventory (NPI) (Cummings *et al.*, 1994).

MRI analysis

The MR images of the brain were acquired with 1.5-T MR imaging, Intera 1.5T Achieve Nova (Philips Medical Systems, Best, the Netherlands). T_1-weighted MR images were obtained at 1-mm slices in 49 of the 53 (92.5%) subjects. The remaining four subjects underwent computed tomography (CT) because of metals in their body. None of the participants showed any significant organic changes on brain imaging. We analyzed the 49 subjects who completed MRI. VSRAD analysis was performed for assessing the severity of atrophic changes in the medial temporal lobe using 3D-T_1-weighted imaging of the entire brain and SPM8 (Statistical Parametric Mapping, 2008 edition) plus DARTEL as described by preceding studies (Matsuda *et al.*, 2012). To calculate the *z*-score in the entorhinal cortex, normalization to global mean intensities was carried out. This step allows correction of the absolute amount of gray matter for individual total brain volumes. The severity of atrophic changes was described as the *z*-score, calculated as *z*-score = ([control mean] − [individual value])/(control SD), where control values came from the imaging database consisting of 40 Japanese men and 40 Japanese women aged between 54 and 86 years (Matsuda *et al.*, 2012).

PET analysis

A PET scanner system, Eminence SET-3000GCT/X (Shimadzu Corp., Kyoto, Japan), was used to measure regional brain radioactivity. Each scan was preceded by a 4-min transmission scan for attenuation correction using 137Cs. Static PET scanning was performed 50 min after intravenous bolus injection of 370 MBq, with a 10-min emission acquisition scan (as dynamic scan with two 5-min frames). Images were reconstructed with an iterative reconstruction algorithm (four iterations, 16 subsets) using a Gaussian filter of 5-mm full width at half maximum and were saved as a series of 128×128 matrices with a voxel size of $2 \times 2 \times 2$ mm. For quantitative analysis of florbetapir-PET images, we used the same method as described in the previous study (Fleisher *et al.*, 2011). Region of interest (ROI) analysis was performed on individual PET images, spatially normalized to Montreal Neurological Institute atlas space using SPM. Mean cortical ROI templates contained six regions—medial orbital frontal, temporal, anterior, and posterior cingulate, parietal lobe, and precuneus—as defined by the Automated Anatomic Labeling Atlas (Tzourio-Mazoyer *et al.*, 2002). Mean cortical and whole-cerebellar ROI templates were applied to all PET scans to calculate mean regional cerebral-to-cerebellar SUVR (Fleisher *et al.*, 2011). The average of these six regions was evaluated as a measure of global mean cortical florbetapir ^{18}F binding.

Statistical analysis

Kruskal–Wallis test with Steel-Dwass test and chi-square test were used for group comparisons. Receiver operating characteristics (ROC) curve analysis allowed us to examine the diagnostic power of the cerebral-to-whole-cerebellar SUVR or *z*-score of the entorhinal cortex against clinical AD and OHC, and the area under the curve (AUC) was calculated. Sensitivity and specificity of florbetapir PET or MRI were calculated at the optimal cutoff point, and sensitivity and specificity of MRI for beta-amyloid in MCI were also calculated. The linear correlation coefficients for a pair of variables were calculated to determine the correlations among brain imaging, age, and cognitive functions. Multiple regression analysis was used for comparisons among SUVR, age, *z*-score in entorhinal cortex, MMSE, and ADAS-Jcog. In all tests, a p value < 0.05 was considered statistically significant. Bonferroni correction was used for multiple comparisons.

Ethics statement

This study was approved by the review board of Nippon Medical School Hospital, Tokyo, Japan (#221038). The study was conducted in accordance with the Declaration

of Helsinki. Study procedures were performed after written informed consent was obtained from the study participants or from authorized representatives of patients with clinical AD.

Results

Background characteristics of the OHC, MCI, and clinical AD groups are shown in Table 1. There were no significant differences between the respective groups in terms of gender and age. MMSE score (mean ± SD) was 18.3 ± 4.6 for the clinical AD group, 26.7 ± 1.8 for the MCI group, and 29.2 ± 1.1 for the OHC group. ADAS-Jcog score (mean ± SD) was 20.4 ± 11.1 for the clinical AD group, 8.9 ± 4.5 for the MCI group, and 4.6 ± 2.6 for the OHC group. NPI score (mean ± SD) was 10.4 ± 11.2 for the clinical AD group, 10.8 ± 11.2 for the MCI group, and 0.8 ± 1.5 for the OHC group. CDR score (mean ± SD) was 1.2 ± 0.7 for the clinical AD group, 0.6 ± 0.2 for the MCI group, and 0.0 ± 0.0 for the OHC group. Average SUVR (mean ± SD) among the three groups (AD, 1.21 ± 0.13; MCI, 1.03 ± 0.15; OHC, 1.04 ± 0.14) was significantly different (Kruskal–Wallis test: $\chi^2 = 15.20$, $df = 2$, $p < 0.001$, Cramer's $V = 0.54$). Average SUVR of the AD group was significantly higher than that of both the MCI and OHC groups in multiple comparisons with Steel-Dwass test (AD vs MCI: $z = -3.21$, $p < 0.001$, $r = -0.52$; AD vs OHC: $z = -3.43$, $p < 0.001$, $r = 0.59$; MCI vs OHC: $z = 0.47$, $p = 0.89$, $r = 0.08$). Average z-score of entorhinal cortex atrophy (mean ± SD) among the three groups (AD, 2.5 ± 1.1; MCI, 1.4 ± 0.8; OHC, 1.3 ± 1.4) was significantly different (Kruskal–Wallis test: $\chi^2 = 14.98$, $df = 2$, $p < 0.001$, Cramer's $V = 0.53$). Average z-score of the AD group was significantly higher than that of both the MCI and OHC groups in multiple comparisons with Steel-Dwass test (AD vs MCI: $z = -2.93$, $p = 0.003$, $r = -0.50$; AD vs OHC: $z = -3.44$, $p < 0.001$, $r = -0.63$; MCI vs OHC: $z = -1.49$, $p = 0.14$, $r = -0.26$).

Analysis of amyloid PET and MRI

Although the clinical reference standard may be imperfect owing to challenges of a differential diagnosis of AD versus other dementias in the AD group, and by potential contamination with pre-clinical AD subjects in the OHC group, the clinical reference standard can still be used to define cutoff points for abnormality. Thus, ROC curve analyses, using the clinical reference standard, were used to confirm the cutoff point for abnormality in amyloid and entorhinal cortex atrophy in this population. The results of ROC curve analyses are shown in Table 2. ROC curve analysis for amyloid PET showed the best sensitivity (84.2%) and specificity (80.0%) with a cutoff value of 1.099 (AUC was 0.849, 95% CI 0.717 to 0.981) for the differential diagnosis of clinical AD from OHC. When using the cutoff value of 1.099, 16 of 19 (84.2%) AD, 7 of 19 (36.8%) MCI, and 3 of 15 (20%) OHC were beta-amyloid positive.

The ROC curve analysis for MRI showed the best sensitivity (86.7%) and specificity (80.0%) values with

Table 1 Background characteristics and results of florbetapir PET and z-score in entorhinal cortex of AD group, MCI group, and OHC group

	N	Sex	Age (years)	MMSE	ADAS-Jcog	CDR	NPI	SUVR	z-score in entorhinal cortex
OHC	15	M 7/F 8	69.9 ± 3.7	29.2 ± 1.1	4.6 ± 2.6	0.0 ± 0.0	0.8 ± 1.5	1.04 ± 0.14	1.3 ± 1.4
AD	19	M 3/F 16	75.7 ± 6.8	18.3 ± 4.6	20.4 ± 11.1	1.2 ± 0.7	10.4 ± 11.2	1.21 ± 0.13	2.5 ± 1.1
MCI	19	M 6/F 13	74.6 ± 6.4	26.7 ± 1.8	8.9 ± 4.5	0.6 ± 0.2	10.8 ± 11.2	1.03 ± 0.15	1.4 ± 0.8

Table 2 Results of ROC curve analysis

	MRI morphometry	[^{18}F]florbetapir PET
Cutoff value	z-score = 1.60	SUVR = 1.099
AD vs OHC		
% of AD positive	86.7	84.2
% of OHC negative	80.0	80.0
Area under curve (95% CI)	0.871 (0.745 to 0.998)	0.849 (0.717 to 0.981)
Number of positive among MCI (%)	6 (31.6)	7 (36.8)

Differential diagnosis of clinical AD from OHC was calculated by using each cutoff value. The number of MCI patients with positive z-score or SUVR was defined by the cutoff value of MRI or [^{18}F]florbetapir.

a cutoff value of 1.60 (AUC was 0.871, 95% CI 0.745 to 0.998) for the differential diagnosis of clinical AD from OHC. When using the cutoff value of 1.60, 13 of 15 (86.7%) AD, 6 of 19 (31.6%) MCI, and 3 of 15 (20%) of OHC were entorhinal cortex atrophy positive.

There was no significant correlation between SUVR and z-score ($r = 0.06$, $p = 0.71$) (Figure 1).

Comparison of abnormalities detected with different imaging biomarkers. The presence of abnormal amyloid defined with SUVR > 1.099 and that of entorhinal cortex atrophy-positive with z-score > 1.60 are compared in Table 3. Thirteen of 22 beta-amyloid-positive subjects were classified as entorhinal cortex atrophy positive (59.1% positive-agreement rate), and 18 of 27 beta-amyloid-negative subjects were classified as entorhinal cortex atrophy negative (66.7% negative-agreement rate). The overall agreement statistic for the presence of these two abnormalities was low ($\kappa = 0.258$, 95% CI −0.0152 to 0.530).

Interestingly, among amyloid-positive clinically diagnosed AD subjects, nearly all (11 of 12) showed entorhinal cortex atrophy (Table 4). The single amyloid-positive AD subject but without entorhinal cortex atrophy was also among the clinically mildest of AD subjects in the study (MMSE = 23, ADAS-Jcog = 12). Amyloid-positive MCI subjects and amyloid-positive OHC subjects showed low rates of entorhinal cortex atrophy (two of seven and zero of three), consistent with earlier clinical stage of the disease.

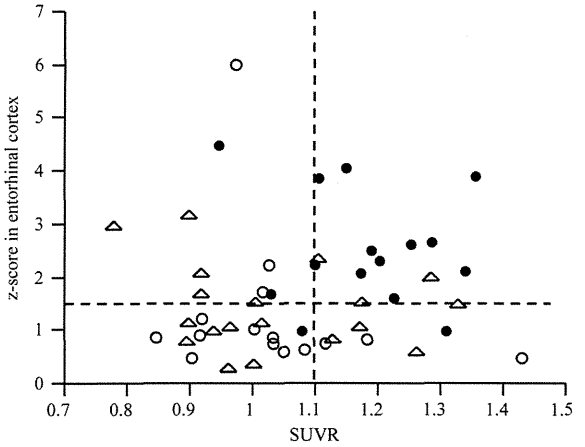

Figure 1 Association between SUVR and z-score in all participants. There was no significant correlation between SUVR and z-score ($r = 0.06$, $p = 0.71$). (•, AD; △, MCI; ○, OHC); dashed lines indicate the cutoff values of SUVR (1.099) and z-score (1.60).

Table 3 Results of group comparison between beta-amyloid and z-score

	Amyloid positive	Amyloid negative	Total
z-score positive (*N*)	13	9	22
z-score negative (*N*)	9	18	27
Total	22	27	49

Four patients with AD did not have MRI data.

Correlation among imaging biomarkers and cognitive function

All participants. There was no significant correlation between SUVR and z-score. MMSE was significantly correlated with age ($r = -0.301$, $p = 0.03$), SUVR ($r = -0.410$, $p < 0.01$), and z-score ($r = -0.459$, $p < 0.01$); and ADAS-Jcog was significantly correlated with SUVR ($r = 0.367$, $p < 0.01$) and z-score ($r = 0.525$, $p < 0.01$). Multiple regression analysis among all participants showed that age, z-score, and SUVR predicted MMSE ($R^2 = 0.39$, $F(3, 45) = 9.41$, $p < 0.01$, $\eta^2 = 0.39$) and ADAS-Jcog ($R^2 = 0.41$, $F(3, 45) = 10.26$, $p < 0.01$, $\eta^2 = 0.41$). z-score and SUVR significantly influenced both MMSE ($F = 8.79$, $p < 0.01$ and $F = 10.25$, $p < 0.01$, respectively) and ADAS-Jcog ($F = 14.09$, $p < 0.01$ and $F = 8.76$, $p < 0.01$, respectively). The results did not change after Bonferroni correction ($p < 0.017 = 0.05/3$).

Subjects with and without beta-amyloid. We divided the AD, MCI, and OHC groups into beta-amyloid positive and beta-amyloid negative by the cutoff value

Table 4 Rates of entorhinal cortex atrophy in amyloid-positive and amyloid-negative subjects (by diagnostic group)

		Entorhinal cortex atrophy	No entorhinal cortex atrophy
AD ($n = 15$)	Amyloid positive ($n = 12$)	11/12 (91.7%)	1/12 (8.3%)
	Amyloid negative ($n = 3$)	2/3 (66.7%)	1/3 (33.3%)
MCI ($n = 19$)	Amyloid positive ($n = 7$)	2/7 (28.6%)	5/7 (71.4%)
	Amyloid negative ($n = 12$)	4/12 (33.3%)	8/12 (66.7%)
OHC ($n = 15$)	Amyloid positive ($n = 3$)	0/3 (0.0%)	3/3 (100.0%)
	Amyloid negative ($n = 12$)	3/12 (25.0%)	p9/12 (75.0%)

Four patients with AD did not have MRI data.

of 1.099. The linear correlation coefficients separately calculated for subjects with and without beta-amyloid are shown in Table 5. SUVR was not significantly correlated with age, MMSE, ADAS-Jcog, or *z*-score in subjects with and without beta-amyloid. Among subjects with beta-amyloid, both MMSE ($r = -0.626$, $p < 0.01$) and ADAS-Jcog ($r = 0.691$, $p < 0.01$) were significantly correlated with *z*-score (Figure 2). Among subjects without beta-amyloid, MMSE was significantly correlated with age ($r = 0.555$, $p < 0.01$), and ADAS-Jcog was significantly correlated with age ($r = 0.522$, $p < 0.01$) and *z*-score ($r = 0.406$, $p = 0.04$). The correlation between ADAS-Jcog and *z*-score among subjects without beta-amyloid became non-significant after Bonferroni correction ($p < 0.025 = 0.05/2$).

Multiple regression analysis in subjects with beta-amyloid revealed that age, *z*-score, and SUVR predicted MMSE ($R^2 = 0.42$, $F(3, 18) = 4.31$, $p = 0.02$, $\eta^2 = 0.42$) and ADAS-Jcog ($R^2 = 0.51$, $F(3, 18) = 6.35$, $p < 0.01$, $\eta^2 = 0.52$). However, only *z*-score significantly influenced both MMSE ($F = 11.90$, $p < 0.01$) and ADAS-Jcog ($F = 17.82$, $p < 0.01$) in subjects with beta-amyloid. Among subjects without beta-amyloid, age, *z*-score, and SUVR predicted MMSE ($R^2 = 0.36$, $F(3, 26) = 4.39$, $p = 0.01$, $\eta^2 = 0.37$) and ADAS-Jcog ($R^2 = 0.35$, $F(3, 26) = 4.19$, $p = 0.02$, $\eta^2 = 0.35$). Only age significantly influenced both MMSE ($F = 10.16$, $p < 0.01$) and ADAS-Jcog ($F = 5.62$, $p = 0.03$). The association between age and ADAS-Jcog among subjects without beta-amyloid became non-significant after Bonferroni correction ($p < 0.017 = 0.05/3$).

Discussion

This is the first study of florbetapir PET in older Japanese subjects. ROC analysis for florbetapir PET revealed that 16 of 19 (84.2%) patients with clinically defined AD, 3 of 15 (20.0%) OHC, and 7 of 19 (36.8%) MCI subjects were classified as beta-amyloid positive. Our results showed that, as expected, AD patients had higher rates of both amyloid positivity and entorhinal cortex

Table 5 Linear correlation coefficients for pairs of variables were calculated to determine the correlations among brain imaging, age, and cognitive functions in subjects with or without beta-amyloid

	MMSE	ADAS-Jcog	MRI morphometry *z*-score	[^{18}F]Florbetapir PET SUVR
Age				
Beta-amyloid (+)	−0.160	0.133	0.383	−0.289
Beta-amyloid (−)	−0.555†	0.522†	0.269	−0.292
MMSE				
Beta-amyloid (+)		−0.850†	−0.626†	−0.086
Beta-amyloid (−)		−0.717†	−0.281	−0.001
ADAS-Jcog				
Beta-amyloid (+)			0.691†	0.093
Beta-amyloid (−)			0.406*	−0.255
z-score				
Beta-amyloid (+)				−0.134
Beta-amyloid (−)				−0.205

*$p < 0.05$, †$p < 0.01$.

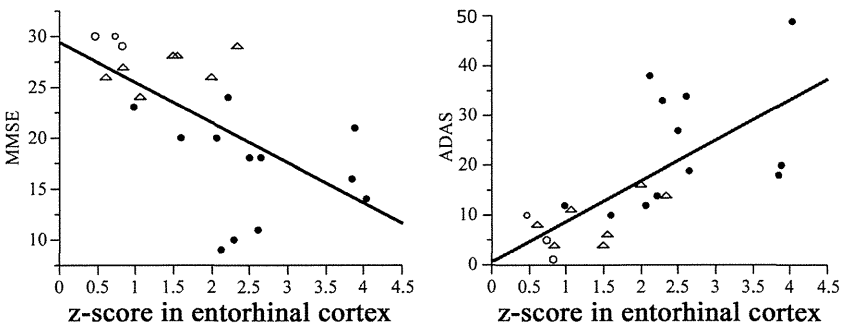

Figure 2 Correlation between cognitive function and volume reduction in entorhinal cortex. *z*-score was significantly correlated with MMSE ($r = -0.626$, $p < 0.01$) and ADAS-Jcog ($r = 0.691$, $p < 0.01$) in patients with beta-amyloid. (•, AD; △, MCI; ○, OHC).

atrophy as compared with OHC. Although both showed similar group differences by ROC analysis, at an individual subject level, PET and MRI revealed important differences. The inconsistency between amyloid PET and MRI may be attributable to the different time courses of these two imaging biomarkers, as repeatedly shown by previous studies (Jack *et al.*, 2008; Jack *et al.*, 2009).

The cutoff value of 1.099 for SUVR in the present study was very comparable with that of previous studies (Fleisher *et al.*, 2011; Camus *et al.*, 2012), and nearly identical to the 1.10 cutoff point prospectively tested by Clark *et al.* (2012), which was shown to have 97% sensitivity and 100% specificity for the detection of AD pathology at autopsy, in a US population. The independent replication of the cutoff point here, using a Japanese cohort, has important implications for the use of amyloid PET tracers in Japanese populations. Furthermore, distribution of beta-amyloid positive was mostly consistent with that in the previous study (clinically defined AD: 84.2% vs 85.3% and 85.0%; MCI: 36.8% vs 46.6% and 50%; OHC: 20.0% vs 28.1% and 60.0%) (Clark *et al.*, 2012), indicating similar rates of amyloid positivity in US and Japanese research populations and suggesting that florbetapir PET can be a useful imaging technique for older Japanese populations.

The most interesting finding in our study was the association between cognitive decline and entorhinal cortex atrophy among subjects with beta-amyloid. Past studies reported that entorhinal cortex atrophy was associated with AD independent of age (Jack *et al.*, 2002) and was significantly correlated with MMSE score (Gosche *et al.*, 2002; Jack *et al.*, 2002), although amyloid PET was not used. In our study, SUVR was not correlated with cognitive decline, but entorhinal cortex atrophy was significantly correlated with cognitive decline in subjects with beta-amyloid. Multiple regression analysis also showed that only entorhinal cortex atrophy was correlated with cognitive decline in subjects with beta-amyloid, whereas only age was correlated with cognitive decline in those without beta-amyloid. A recent study examined the association between cognitive function and both [^{18}F]FDG and [^{18}F]florbetapir PET, reporting that MMSE score was correlated only with uptake of [^{18}F]FDG PET, not [^{18}F]florbetapir PET, in AD (Newberg *et al.*, 2012). Another study reported that MRI had a closer relationship with cognitive performance later in the disease than other biomarkers (Becker *et al.*, 2011). It has also been reported that the association between the accumulation of beta-amyloid and cognitive function was not straightforward, as the accumulation of beta-amyloid might plateau, leading to a "ceiling effect" relatively early in the disease process that would confound linear correlations between plaque number and severity of cognitive change (Ingelsson *et al.*, 2004). Our result that the frequency of beta-amyloid positive was increased in the following order: OHC, MCI, and clinical AD; but cognitive impairment was not correlated with the accumulation of beta-amyloid, was consistent with the hypothetical model of the progress of AD, and might also support the existence of this ceiling effect. Thus, our result that only volume reduction in the entorhinal cortex was correlated with cognitive function among subjects with beta-amyloid indicated that [^{18}F] florbetapir PET was suitable for the diagnosis of AD pathology, and MRI morphometry was suitable for evaluation of the severity of clinical AD.

We should acknowledge several methodological limitations in our study. First, the sample size was relatively small, as this study was conducted only in our institution and was the first clinical research of florbetapir PET in Japan. Thus, the findings may not pertain to other populations or groups. A future study with a larger number of participants would be meaningful. Second, use of the whole cerebellum as reference region for SUVR calculations has not been proven to be superior to other noncortical brain regions, such as the pons or cerebellar gray matter. A whole cerebellar reference region was chosen here because it rarely contains fibrillar amyloid plaques, and cortical regions on PET scans typically contain a mixture of white and gray matter tissue, which is matched by the whole cerebellar region. Therefore, theoretically, the whole cerebellum should be a suitable measure of neutral nonspecific florbetapir binding (Joachim *et al.*, 1989; Choi *et al.*, 2009). Third, the process of neurodegeneration of AD may start from the entorhinal cortex and then progressing to the whole brain. Voxel-based morphometry with diffeomorphic anatomical registration through exponentiated Lie algebra might be superior to visual inspection. However, we cannot rule out the possibility of atrophic change of the whole brain influencing our results. Fourth, four subjects did not undergo MRI because of metals in their body. Newly developed CT-based morphometry, which showed usefulness similar to MRI-based morphometry (Imabayashi *et al.*, 2013), might help such subjects in the future. Fifth, we did not know the APOE genotype of the participants, and therefore, we could not know its effect on the results of our study. APOE genotype is known to be not only a risk factor for AD but also that it affects the levels of beta-amyloid plaque deposition and atrophic brain changes (Drzezga *et al.*, 2009).

In conclusion, this is the first study to compare [^{18}F]florbetapir PET and MRI voxel-based analysis for

AD. Both [^{18}F]florbetapir PET and MRI morphometry detected changes in AD as compared with OHC. However, these two different imaging biomarkers did not correlate with each other, and diagnoses based on the different imaging biomarkers were inconsistent. This inconsistency might be attributable to the different roles of amyloid PET and MRI morphometry, that is, amyloid PET detects the accumulation of beta-amyloid occurring early in AD, and MRI morphometry for subjects with beta-amyloid detects entorhinal cortex atrophy that is closely related to cognitive decline and occurs later in AD. Thus, [^{18}F]florbetapir PET makes it possible to detect AD pathology in the early stage of the disease, whereas MRI morphometry for subjects with beta-amyloid provides a good biomarker for assessing the severity of AD in the later stage.

Conflict of interest

All authors have read the journal's policy and have the following statement. Y. O. has received speaker's honoraria from Dainippon Sumitomo Pharma, GlaxoSmithKline, Janssen Pharmaceutical, Otsuka, Pfizer, Eli Lilly, Astellas, Yoshitomi, and Meiji within the past 3 years. H. S. has received speaker's honoraria from Pfizer and Eisai within the past 3 years. M. M. and D. S. are current employees of Avid Radiopharmaceuticals Inc. The radiotracer was provided at no cost to the study by Avid Radiopharmaceuticals Inc. For the remaining authors, none was declared, and there were no other relationships or activities that could appear to have influenced the submitted work.

Key points

- When using a cutoff value for [^{18}F]florbetapir PET (1.099 for SUVR), 16 of 19 (84.2%) AD, 7 of 19 (36.8%) MCI, and 3 of 15 (20.0%) OHC were beta-amyloid positive.
- MRI morphometry with VSRAD was just as useful as amyloid imaging for differential diagnosis of clinical AD (i.e., sensitivity of 84.2% and specificity of 80.0% for amyloid PET, sensitivity of 86.7% and specificity of 80.0% for MRI).
- Entorhinal cortex atrophy detected by MRI with VSRAD significantly correlated with cognitive decline only in subjects with beta-amyloid.
- [^{18}F]florbetapir PET makes it possible to detect AD pathology in the early stage of the disease, whereas MRI morphometry for subjects with beta-amyloid provides a good biomarker for assessing the severity of AD in the later stage.

Acknowledgements

We thank Koji Nagaya, Koji Kanaya, Masaya Suda, Megumi Takei, and Minoru Sakurai (Clinical Imaging Center for Healthcare, Nippon Medical School, Tokyo, Japan) for their assistance in performing the PET experiments and MRI scanning. We also thank Michihiko Koeda for advice on the statistics.

This study was partly supported by a Grant-in-Aid for Scientific Research (B) from the Ministry of Education, Culture, Sports, Science and Technology (MEXT), Japanese government (2011–2015); by a grant of Strategic Research Foundation Grant-aided Project for Private Universities from the Ministry of Education, Culture, Sport, Science, and Technology, Japan (MEXT) (2008–2012); and by a Health and Labor Sciences Research Grant for Research on Psychiatric and Neurological Diseases and Mental Health from the Ministry of Health, Labor and Welfare, Japanese government. The funders had no role in the study design, data collection and analysis, decision to publish, or preparation of the manuscript.

Author contributions

A. T. conceived the study, collected imaging and clinical data, performed the analysis, and drafted the manuscript. T. S. and Y. K. collected and interpreted the clinical data. M. H., T. S., and S. M. assisted in the study design and revised the manuscript draft. M. M. and D. S. assisted in interpretation of imaging data and revised the manuscript draft. K. H., K. I., and S. K. collected imaging data and revised the manuscript draft. H. S. and Y. O. assisted in data collection, infrastructure, and revising the manuscript draft.

References

Becker JA, Hedden T, Carmasin J, *et al.* 2011. Amyloid-beta associated cortical thinning in clinically normal elderly. *Ann Neurol* **69**: 1032–1042.

Camus V, Payoux P, Barré L, *et al.* 2012. Using PET with 18F-AV-45 (florbetapir) to quantify brain amyloid load in a clinical enviroment. *Eur J Nucl Med Mol Imaging* **39**: 621–631.

Choi SR, Golding G, Zhuang Z, *et al.* 2009. Preclinical properties of 18F-AV-45: a PET agent for Abeta plaques in the brain. *J Nucl Med* **50**: 1887–1894.

Clark CM, Schneider JA, Bedell BJ, *et al.* 2011. Use of florbetapir-PET for imaging beta-amyloid pathology. *JAMA* **305**: 275–283.

Clark CM, Pontecorvo MJ, Beach TG, *et al.* 2012. Cerebral PET with florbetapir compared with neuropathology at autopsy for detection of neuritic amyloid-beta plaques: a prospective cohort study. *Lancet Neurol* **11**: 669–678.

Cummings JL, Mega M, Gray K, *et al.* 1994. The Neuropsychiatric Inventory: comprehensive assessment of psychopathology in dementia. *Neurology* **44**: 2308–2314.

Drzezga A, Grimmer T, Henriksen G, *et al.* 2009. Effect of APOE genotype on amyloid plaque load and gray matter volume in Alzheimer disease. *Neurology* **72**: 1487–1494.

Fleisher AS, Chen K, Liu X, *et al.* 2011. Using positron emission tomography and florbetapir F 18 to image cortical amyloid in patients with mild cognitive impairment or dementia due to Alzheimer disease. *Arch Neurol* **68**: 1404–1411.

Folstein MF, Folstein SE, McHugh PR. 1975. "Mini-mental state". A practical method for grading the cognitive state of patients for the clinician. *J Psychiatr Res* **12**: 189–198.
Gosche KM, Mortimer JA, Smith CD, *et al.* 2002. Hippocampal volume as an index of Alzheimer neuropathology: findings from the Nun Study. *Neurology* **58**: 1476–1482.
Hirata Y, Matsuda H, Nemoto K, *et al.* 2005. Voxel-based morphometry to discriminate early Alzheimer's disease from controls. *Neurosci Lett* **382**: 269–274.
Homma A, Fukuzawa K, Tsukada Y, *et al.* 1992. Development of a Japanese version of Alzheimer's Disease Assessment Scale (ADAS). *Jpn J Geriatr Psychiatry* **3**: 647–655. Japanese
Imabayashi E, Matsuda H, Tabira T, *et al.* 2013. Comparison between brain CT and MRI for voxel-based morphometry of Alzheimer's disease. *Brain Behav* **3**: 487–493.
Ingelsson M, Fukumoto H, Newell KL, *et al.* 2004. Early Abeta accumulation and progressive synaptic loss, gliosis, and tangle formation in AD brain. *Neurology* **62**: 925–931.
Jack CR Jr, Dickson DW, Parisi JE, *et al.* 2002. Antemortem MRI findings correlate with hippocampal neuropathology in typical aging and dementia. *Neurology* **58**: 750–757.
Jack CR Jr, Lowe VJ, Senjem ML, *et al.* 2008. ^{11}C PiB and structural MRI provide complementary information in imaging of Alzheimer's disease and amnestic mild cognitive impairment. *Brain* **131**: 665–680.
Jack CR Jr, Lowe VJ, Weigand SD, *et al.* 2009. Serial PiB and MRI in normal, cognitive impairment and Alzheimer's disease: implications for sequence of pathological events in Alzheimer's disease. *Brain* **132**: 1355–1365.
Jack CR Jr, Knopman DS, Jaqust WJ, *et al.* 2010. Hypothetical model of dynamic biomarkers of the Alzheimer's pathological cascade. *Lancet Neurol* **9**: 119–128.
Joachim CL, Morris JH, Selkoe DJ. 1989. Diffuse senile plaques occur commonly in the cerebellum in Alzheimer's disease. *Am J Pathol* **135**: 309–319.
Kemppainen NM, Aalto S, Wilson IA, *et al.* 2006. Voxel-based analysis of PET amyloid ligand [^{11}C]PIB uptake in Alzheimer disease. *Neurology* **67**: 1575–1580.
Klunk WE, Engler H, Nordberg A, *et al.* 2004. Imaging brain amyloid in Alzheimer's disease with Pittsburgh compound-B. *Ann Neurol* **55**: 306–319.
Matsuda H, Mizumura S, Nemoto K, *et al.* 2012. Automatic voxel-based morphometry of structural MRI by SPM8 plus diffeomorphic anatomic registration through exponentiated Lie algebra improves the diagnosis of probable Alzheimer disease. *AJNR Am J Neuroradiol* **33**: 1109–1114.
McKhann G, Drachman D, Folstein M, *et al.* 1984. Clinical diagnosis of Alzheimer's disease: report of the NINCDS-ADRDA Work Group under the auspices of Department of Health and Human Services Task Force on Alzheimer's disease. *Neurology* **34**: 939–944.
Morris JC. 1993. The Clinical Dementia Rating (CDR): current version and scoring rules. *Neurology* **43**: 2412–2414.
Maruyama M, Shimada H, Suhara T, *et al.* 2013. Imaging of tau pathology in tauopathy mouse model and in Alzheimer patients compared to normal controls. *Neuron* **18**: 1094–1108.
Nagata T, Shinagawa S, Ochiai Y, *et al.* 2011. Association between executive dysfunction and hippocampal volume in Alzheimer's disease. *Int Psychogeriatr* **23**: 764–771.
Newberg AB, Arnold SE, Wintering N, *et al.* 2012. Initial clinical comparison of ^{18}F-florbetapir and ^{18}F-FDG PET in patients with Alzheimer disease and controls. *J Nucl Med* **53**: 902–907.
Rinne JO, Någren K. 2010. Positron emission tomography in at risk patients and in the progression of mild cognitive impairment to Alzheimer's disease. *J Alzheimers Dis* **19**: 291–300.
Scheltens P, Fox N, Barkhof F, De Carli C. 2002. Structural magnetic resonance imaging in the practical assessment of dementia: beyond exclusion. *Lancet Neurol* **1**: 13–21.
Shibuya Y, Kawakatsu S, Hayashi H, *et al.* 2013. Comparison of entorhinal cortex atrophy between early-onset and late-onset Alzheimer's disease using the VSRAD, a specific and sensitive voxel-based morphometry. *Int J Geriatr Psychiatry* **28**: 372–376.
Tzourio-Mazoyer N, Landeau B, Papathanassiou D, *et al.* 2002. Automated anatomical labeling of activations in SPM using a macroscopic anatomical parcellation of the MNI MRI single-subject brain. *Neuroimage* **15**: 273–289.

RESEARCH ARTICLE

International Journal of Geriatric Psychiatry

Amyloid imaging with [^{18}F]florbetapir in geriatric depression: early-onset versus late-onset

Amane Tateno[1], Takeshi Sakayori[1], Makoto Higuchi[2], Tetsuya Suhara[2], Keiichi Ishihara[3], Shinichiro Kumita[4], Hidenori Suzuki[5] and Yoshiro Okubo[1]

[1]Department of Neuropsychiatry, Nippon Medical School, Bunkyo-ku, Tokyo, Japan
[2]Molecular Imaging Center, National Institute of Radiological Sciences, Chiba, Japan
[3]Clinical Imaging Center for Healthcare, Nippon Medical School, Bunkyo-ku, Tokyo, Japan
[4]Department of Radiology, Nippon Medical School, Bunkyo-ku, Tokyo, Japan
[5]Department of Pharmacology, Nippon Medical School, Bunkyo-ku, Tokyo, Japan
Correspondence to: Y. Okubo, MD, PhD, E-mail: okubo-y@nms.ac.jp

Background: We examined patients with mild cognitive impairment (MCI) with a history of geriatric depression (GD) and healthy controls (HC) to evaluate the effect of beta-amyloid (Aβ) pathology on the pathology of GD by using [^{18}F]florbetapir PET.

Methods: Thirty-three elderly patients (76.7 ± 4.2 years) and 22 healthy controls (HC; 72.0 ± 4.5 years, average ± SD) were examined by [^{18}F]florbetapir positron emission tomography (PET) to quantify the standard uptake value ratio (SUVR) as the degree of amyloid accumulation, by MRI to determine the degree of atrophy, by Mini-Mental State Examination for cognitive functions, and by Geriatric Depression Scale for the severity of depression, and by Clinical Dementia Rating for activity of daily living (ADL). The cut-off value of 1.08 for SUVR was defined as Aβ-positive.

Results: Of the patients and HC, 39.4% and 27.3%, respectively, were beta-amyloid-positive. The onset age of GD was significantly correlated with SUVR ($r = 0.44$, $p < 0.01$). Compared to patients without Aβ (GD-Aβ), patients with Aβ (GD + Aβ) did not differ in terms of age, cognitive function, severity of depression and ADL, and brain atrophy. GD + Aβ had significantly older average ± SD age at onset of GD (73.6 ± 7.1 versus 58.7 ± 17.8, $p < 0.01$) and significantly shorter average ± SD time between onset of GD and PET scan day (3.1 ± 5.2 years versus 18.1 ± 18.6 years, $p < 0.001$) than GD-Aβ.

Conclusions: Our results showed that the rate of Aβ positivity was higher in late-onset GD and that onset-age was associated with SUVR, suggesting that the later the onset of GD, the more Aβ pathology affected its onset. Copyright © 2014 John Wiley & Sons, Ltd.

Key words: geriatric depression; beta-amyloid; Alzheimer's disease; positron emission tomography
History: Received 16 June 2014; Revised 19 August 2014; Accepted 19 August 2014; Published online in Wiley Online Library (wileyonlinelibrary.com)
DOI: 10.1002/gps.4215

Introduction

Abundant evidence has pointed to a strong link between depression and dementia. Previous studies have indicated that depression was associated with an increased risk of developing dementia, Alzheimer type (AD) (Ownby *et al.*, 2006), and depression that may occur in more than 20% of patients with AD (Starkstein *et al.*, 2011). Many studies have reported that both early-onset depression and late-onset depression are risk factors for subsequence dementia (Geerlings *et al.*, 2008). Vascular disease, increased levels of glucocorticoids, and chronic inflammation were thought to be possible common mechanisms for depression and AD (Byers and Yaffe, 2011). However, the nature of this association still remains a matter of debate, that is, whether depression is a risk factor or prodrome, or a consequence of AD, and whether depression and AD share the same mechanism.

Another factor possibly underlying the association between AD and depression is amyloid and tau protein. Recent advances in positron emission tomography (PET) and radioligands have allowed us to visualize the accumulation of Aβ or tau protein in vivo. Some previous studies reported that patients with late-life depression showed significantly higher [18F]FDDNP binding, which indicated the presence of beta-amyloid (Aβ) and tau protein, by PET in the posterior cingulate and lateral temporal regions compared to controls (Kumar *et al.*, 2011), and elderly patients with major depression showed significantly lower cerebrospinal fluid beta-amyloid 42 than controls (Pomara *et al.*, 2012). A recent study revealed that 33% of cognitively normal young and middle-aged subjects showed hyperphosphorylated tau pathology in the transentorhinal cortex and/or the locus coeruleus (Elobeid *et al.*, 2012). Neuritic plaques and neurofibrillary tangles are more pronounced in the hippocampus of AD patients with comorbid depression as compared with AD patients without depression (Rapp *et al.*, 2008). These findings, taken together, support the concept of amyloid-associated depression. Amyloid-associated depression has been proposed to explain the subtype of depression representing a prodromal of AD (Sun *et al.*, 2008). Although a previous study reported that the cortical Aβ level did not differ between patients with lifetime history of major depressive episodes (MDE) and healthy controls (Madsen *et al.*, 2008), a more recent study using [^{18}F]florbetapir reported that cognitively normal patients with late-life major depression showed higher standard uptake value ratio (SUVR) in the precuneus and parietal region than healthy controls (Wu *et al.*, 2014). [^{18}F]florbetapir is a radioligand that distinctly detects the accumulation of Aβ in vivo. We recently reported the usefulness of [^{18}F]florbetapir as a biomarker of AD (Tateno *et al.*, 2014). However, the same study by Wu *et al.* (2014) did not find any association between global SUVR and prior depression episodes, age at onset of depression, or time since onset of first depression. Another study also reported that the severity of depression was not associated with higher phosphorylated tau 181 and total tau or reduced beta-amyloid 1–42 in AD or non-demented subjects (Kramberger *et al.*, 2012). Thus, the association between Aβ and depression is still a matter of debate.

In this study, we examined patients with mild cognitive impairment (MCI) with a history of geriatric depression (GD) and healthy controls (HC) to evaluate the effect of Aβ pathology on the pathology of GD by using [^{18}F]florbetapir PET. If the Aβ pathology affects the pathology of GD, the characteristics of these patients might differ from those of GD without Aβ pathology.

Materials and methods

Participants

The patient group consisted of men and women aged 70 years or older who met the criteria of MCI as defined by Petersen and Morris (Petersen and Morris, 2005). All of them were amnestic MCI. They also had a history of MDE based on the Diagnostic and Statistical Manual of Mental Disorder 4th edition, text revision. All of them were patients at our hospital. For confirmation of the presence of a past history of major depressive episodes before 2000, we checked the patients' medical records to see whether their symptoms were applied to the diagnosis of major depressive episode by DSM-IV-TR. All of them had at least 1 MDE after the age of 65 years. The healthy control group (HC) consisted of men and women aged 65 years or older who were without subjective cognitive dysfunction, dysfunction of activity of daily living (ADL), and past or current history of psychiatric illness. HC were also interviewed to assess any current and past history of psychiatric illness. Exclusion criteria were other current clinically relevant neurologic or ischemic illness, history of apparent brain injury, or having ever undergone anti-amyloid experimental therapy. A total of 33 patients with MCI and a history of MDE (76.7 ± 4.2 years old, mean ± SD, 29 females and 4 males) and 22 HC (72.0 ± 4.5 years old, mean ± SD, 10 females and 12 males) participated in this study. All of the patients with MCI and a history of MDE were continuing to take medications at the time of examination and 16 of 33 (48.5%) met the criteria of MDE at the time of examination. Twenty-one of the patients (63.6%) and 10 HC (45.5%) were examined for APOE phenotype. Current history of hypertension, hyperlipidemia, and diabetes mellitus was investigated for the evaluation of cardiovascular risk factors.

Neuropsychiatric assessment

Their cognitive function was evaluated by Mini-Mental State Examination (MMSE) (Folstein *et al.*, 1975). ADL was measured by Clinical Dementia Rating (CDR) (Morris, 1993), and depression severity was assessed by Geriatric Depression Scale (GDS) (Sheikh and Yesavage, 1986).

MRI analysis

We used the same method as in our previous study (Tateno *et al.*, 2014). MR images of the brain were acquired with 1.5T MR imaging, Intera 1.5T Achieve Nova (Philips Medical Systems, Best, Netherlands). T_1-weighted MR images were obtained at 1-mm slices for 30 of the 33 (90.9%) patients and all HC; the other three patients had metal in their bodies. Voxel-based specific regional analysis for AD (VSRAD) was used for assessing the severity of atrophic changes in the entorhinal cortex using 3D-T_1-weighted images of the entire brain and SPM8 (Statistical Parametric Mapping, 2008 edition) as described in previous studies (Hirata *et al.*, 2005). The severity of atrophic changes in the entorhinal cortex was described by *z*-score (Hirata *et al.*, 2005).

We used the Fazekas scale for cerebral white matter lesions (i.e. periventricular hyperintensity (PVH), deep subcortical and white matter hyperintenstiy (DSWMH)) to evaluate vascular factors on MRI (Fazekas *et al.*, 1991). We also evaluated the presence of lacunar infarction.

PET analysis

A PET scanner system, Eminence SET-3000GCT/X (Shimadzu Corp., Kyoto, Japan), was used to measure regional brain radioactivity. Each scan was preceded by a 4-min transmission scan for attenuation correction using 137Cs. Static PET scanning, 10-min emission acquisition (dynamic scan with two 5-min frames), was performed 50 min after intravenous bolus injection of 370 MBq. Images were reconstructed with an iterative reconstruction algorithm (4 iterations, 16 subsets) using a Gaussian filter at 5-mm full-width at half-maximum, and were saved as a series of 128×128 matrices with a voxel size of $2 \times 2 \times 2$ mm.

We used the same method as in our previous study (Tateno *et al.*, 2014). For quantitative analysis of the florbetapir-PET images, we used the method of a previous study (Fleisher *et al.*, 2011). Region-of-interest (ROI) analysis was performed on individual PET images, which were spatially normalized to the Montreal Neurological Institute (MNI) atlas space using SPM. Mean cortical ROI templates contained six regions (medial orbital frontal, temporal, anterior, and posterior cingulate, parietal lobe, and precuneus) as defined by the Automated Anatomic Labeling Atlas (Tzourio-Mazoyer *et al.*, 2002). Mean cortical and whole-cerebellar ROI templates were applied to all PET scans to calculate mean regional cerebral-to-cerebellar SUVRs (Fleisher *et al.*, 2011). The average of these six regions was evaluated as a measure of global mean cortical florbetapir F18 binding. A threshold of SUVR greater than 1.08 was used to signify positive Aβ (Fleisher *et al.*, 2011).

Statistical analysis

Wilcoxon test with Steel–Dwass test and chi-square test were used for group comparisons (Fisher's exact test if sample size was prohibitively small). The linear correlation coefficients for pairs of variables were calculated for the correlations between onset age of MDE and SUVR. Receiver operating characteristics (ROC) curve analysis allowed us to examine the diagnostic power of the onset age of MDE or time since the onset of MDE against Aβ, and the area under the curve (AUC) was calculated. In all tests, a probability value <0.05 was considered statistically significant. Bonferroni correction was used for multiple comparisons. Statistical analysis of data was carried out using JMP 8.0.2 (SAS Inc., Cary, NC) on Windows 7.

Ethics statement

This study was approved by the review board of Nippon Medical School Hospital, Tokyo, Japan (#221038). The study was conducted in accordance with the Declaration of Helsinki. Study procedures were performed after written informed consent was obtained from the study participants.

Results

Comparison of patients with history of MDE and healthy subjects

The results were summarized in Table 1. Mean ± SD age at onset of MDE was 64.6 ± 16.2 years, average ± SD duration after onset of first MDE was 12.2 ± 16.4 years, and average ± SD number of MDE was 2.2 ± 1.2. The onset age of MDE was correlated with SUVR ($r = 0.44$, $p = 0.01$) (Figure 1), but was not correlated with *z*-score in the entorhinal cortex ($r = 0.12$, $p = 0.53$). The results did not change after Bonferroni correction ($p < 0.025 = 0.05/2$).

Compared to the patients, HC had significantly higher mean ± SD MMSE score (28.3 ± 1.9 versus 23.7 ± 3.5, $z = 4.81$, $p < 0.01$, $r = 0.65$), CDR score (0.5 ± 0.2 versus 0.0 ± 0.0, $z = -6.28$, $p < 0.001$,

Table 1 Comparison of patients with GD and healthy controls

	GD	HC	*p*-value
N (f/m)	33 (29/4)	22 (10/12)	0.002
Age (years), mean ± SD	76.7 ± 4.2	72.0 ± 4.5	0.001
Hypertension, *N* (%)	17 (51.5)	3 (13.6)	0.005
Hyperlipidemia, *N* (%)	12 (36.4)	1 (4.6)	0.009
Diabetes mellitus, *N* (%)	5 (15.2)	0 (0.0)	0.06
Frequency of current MDE, *N* (%)	16(48.5)	N/A	
Onset age of MDE (years), mean ± SD	64.6 ± 16.2	*N*/A	
Time since onset of MDE (years), mean ± SD	12.2 ± 16.4	N/A	
Number of MDE, mean ± SD	2.2 ± 1.2	N/A	
z-score of entorhinal cortex, mean ± SD	1.3 ± 0.7	1.2 ± 1.2	0.08
SVUR, mean ± SD	1.07 ± 0.16	1.08 ± 0.15	0.90
Number of beta-amyloid positive, *N* (%)	13 (39.4)	6 (27.3)	0.40
Presence of lacunar infarction, *N* (%)	27 (90.0)	20 (90.9)	0.26
Fazekas scale, *N* (%)			
PVH			0.71
Grade 0	5 (16.7)	2 (9.1)	
Grade I	18 (60.0)	15 (68.2)	
Grade II	7 (23.3)	5 (22.7)	
Grade III	0 (0.0)	0 (0.0)	
DSWMH			0.07
Grade 0	2 (6.7)	6 (27.3)	
Grade 1	21 (70.0)	14 (63.6)	
Grade 2	7 (23.3)	5 (9.1)	
Grade 3	0 (0.0)	0 (0.0)	
MMSE, mean ± SD	23.7 ± 3.5	28.3 ± 1.9	0.01
CDR, mean ± SD	0.5 ± 0.2	0.0 ± 0.0	0.001
GDS, mean ± SD	7.0 ± 3.9	1.9 ± 1.8	0.001
Number of APOE E4, *N* (%)	6 (28.6)	1 (10.0)	0.38

GD, patients with geriatric depression; HC, healthy controls; MDE, major depressive episode; SUVR, standard uptake value ratio; PVH, Periventricular hyperintensity; DSWMH, Deep and subcortical white matter hyperintensity; MMSE, Mini-Mental State Examination; CDR, Clinical Dementia Rating; GDS, Geriatric Depression Scale

$r = -0.85$), and GDS score (7.0 ± 3.9 versus 1.9 ± 1.8, $z = -4.65$, $p < 0.001$, $r = -0.63$). There was no significant difference between HC and patients in mean ± SD *z*-score of the entorhinal cortex (1.2 ± 1.2 versus 1.3 ± 0.7, $z = -1.74$, $p = 0.08$, $r = -0.24$) and average ± SD SUVR (1.08 ± 0.15 versus 1.07 ± 0.16, $z = 0.13$, $p = 0.90$, $r = 0.02$). The rate of Aβ-positivity was higher among patients than HC, but the difference did not reach statistical significance (39.4% (13 of 33) versus 27.3% (6 of 22), Fisher's exact test, $p = 0.40$, Cramer's $V = 0.13$). The frequency of APOE E4 was not significantly different between patients and HC (6 of 21 (28.6%) versus 1 of 10 (10.0%), Fisher's exact test $p = 0.38$, Cramer's $V = 0.21$).

The frequencies of current histories of hypertension and hyperlipidemia were significantly higher among the depression group than the healthy control group (51.5% versus 13.6%, Fisher's exact test, $p = 0.005$, Cramer's $V = 0.39$ and 36.4% versus 4.6%, Fisher's exact test, $p = 0.009$, Cramer's $V = 0.37$). The frequency of current history of diabetes mellitus was higher among the depression group than the healthy control group (15.2% versus 0.0%, Fisher's exact test, $p = 0.06$, Cramer's $V = 0.26$).

The frequency of the presence of lacunar infarction was 27 (90.0%) for GD and 20 (90.9%) for HC. For the severity of PVH, GD (grade 0 was 5 (16.7%), grade I was 18 (60.0%), grade II was 7 (23.3%)) was not significantly different from HV (grade 0 was 2 (9.1%), grade I was 15 (68.2%), grade II was 5 (22.7%))

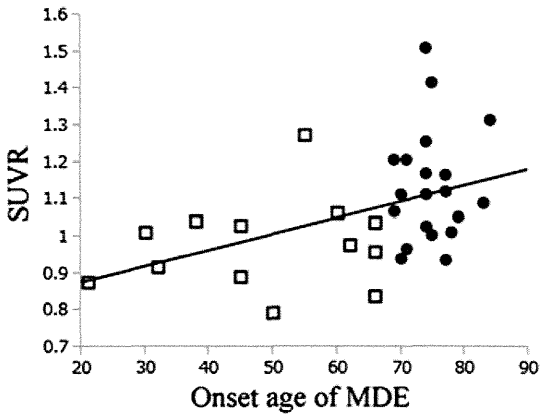

Figure 1 Correlation between standard uptake value (SUVR) of [^{18}F] florgetapir PET and onset age of major depressive episode (MDE). ($r = 0.44$, $p < 0.01$) (•: late-onset geriatric depression, □: early-onset geriatric depression).

($p = 0.71$). For the severity of DSWMH, GD (grade 0 was 2 (6.7%), grade 1 was 21 (70.0%), grade 2 was 7 (23.3%)) was not significantly different from HV (grade 0 was 6 (27.3%), grade 1 was 14 (63.6%), and grade 2 was 5 (9.1%)) ($p = 0.08$).

Comparison of patients with and without beta-amyloid

We then divided the patients into groups with GD and Aβ (GD + Aβ) and without Aβ (GD-Aβ) by the results of amyloid-PET to examine the effect of Aβ pathology on the pathology of GD. The results of group comparisons of GD + Aβ and GD-Aβ are shown in Table 2. There were no significant differences between GD + Aβ and GD-Aβ in the frequency of gender (1 male and 12 females versus 3 males and 17 females, Fisher's exact test $p = 1.00$, Cramer's $V = 0.11$), average ± SD age (76.6 ± 3.9 versus 76.8 ± 4.5, $z = 0.00$; $p = 1.00$, $r = 0.00$), frequency of current MDE (6 of 13 (46.2%) versus 10 of 20 (50.0%), Fisher's exact test $p = 1.00$, Cramer's $V = 0.04$), average ± SD score of MMSE (23.5 ± 3.8 versus 23.8 ± 3.4, $z = -0.09$; $p = 0.91$, $r = -0.02$), CDR (0.6 ± 0.3 versus 0.5 ± 0.2, $z = 0.86$; $p = 0.37$, $r = 0.15$), GDS (6.3 ± 4.6 versus 7.4 ± 3.4, $z = -0.93$; $p = 0.35$, $r = -0.16$), the severity of atrophic changes in the entorhinal cortex (1.5 ± 0.9 versus 1.1 ± 0.6, $z = 0.93$; $p = 0.34$, $r = 0.17$), and the frequency of APOE E4 (3 of 8 versus 3 of 13, Fisher's exact test $p = 0.63$, Cramer's $V = 0.16$). Two patients with GD + Aβ and 1 patient with GD-Aβ, who were not examined by MRI, were excluded only from the analysis using MRI data. Three patients with GD + Aβ and 2 patients with GD-Aβ showed a CDR score of 1.0 because of the negative effect of depression on their function. A list of the medications is shown in Table 3.

The average ± SD onset age of MDE was significantly higher in GD + Aβ than in GD-Aβ (73.6 ± 7.1 versus 58.7 ± 17.8, $z = 2.60$; $p = 0.009$, $r = 0.45$), and the average ± SD time since the onset of first MDE and the PET scan day was significantly shorter in GD + Aβ than in GD- Aβ (3.1 ± 5.2 years versus 18.1 ± 18.6 years, $z = -3.39$; $p < 0.001$, $r = -0.59$). The average ± SD number of MDE was significantly greater in GD-Aβ than in GD + Aβ (2.6 ± 1.4 versus 1.5 ± 0.5, $z = -2.15$; $p = 0.03$, $r = -0.38$); however, the number of MDE became non-significant after Bonferroni correction ($p < 0.025 = 0.05/2$). There was no significant difference between GD + Aβ and GD-

Table 2 Clinical characteristics of patients with and without beta-amyloid

	GD + Aβ	GD-Aβ	*p* value
N (f/m)	13 (12/1)	20 (17/3)	1.00
Age (years), mean ± SD	76.6 ± 3.9	76.8 ± 4.5	1.00
Hypertension, *N* (%)	8 (61.5)	9 (45.0)	0.35
Hyperlipidemia, *N* (%)	5 (38.5)	7 (35.0)	0.84
Diabetes mellitus, *N* (%)	1 (7.7)	4 (20.0)	0.34
Frequency of current MDE, *N* (%)	6 (46.2)	10 (50.0)	1.00
Onset age of MDE (years), mean ± SD	73.6 ± 7.1	58.7 ± 17.8	0.009
Time since onset of MDE (years), mean ± SD	3.1 ± 5.2	18.1 ± 18.6	<0.001
Number of MDE, mean ± SD	1.5 ± 0.5	2.6 ± 1.4	0.03
z-score of entorhinal cortex, mean ± SD	1.5 ± 1.0	1.1 ± 0.6	0.34
Presence of lacunar infarction, *N* (%)	9 (81.8)	18 (94.7)	0.26
Fazekas scale, *N* (%)			
PVH			0.38
Grade 0	1 (9.1)	4 (21.1)	
Grade I	6 (54.6)	12 (63.2)	
Grade II	4 (36.4)	3 (15.8)	
Grade III	0 (0.0)	0 (0.0)	
DSWMH			0.07
Grade 0	1 (9.1)	1 (5.3)	
Grade 1	5 (45.5)	16 (84.2)	
Grade 2	5 (45.5)	2 (10.5)	
Grade 3	0 (0.0)	0 (0.0)	
MMSE, mean ± SD	23.5 ± 3.8	23.8 ± 3.4	0.91
CDR, mean ± SD	0.6 ± 0.3	0.5 ± 0.2	0.37
GDS, mean ± SD	6.3 ± 4.6	7.4 ± 3.4	0.35
N of APOE E4, *N* (%)	3 (37.5)	3 (23.1)	0.63

GD + Aβ, MCI patients with geriatric depression and beta-amyloid; GD-Aβ, MCI patients with geriatric depression without beta-amyloid; MDE, major depressive episode; Aβ, beta-amyloid; PVH, Periventricular hyperintensity; DSWMH, Deep and subcortical white matter hyperintensity; MMSE, Mini-Mental State Examination; CDR, Clinical Dementia Rating; GDS, Geriatric Depression Scale